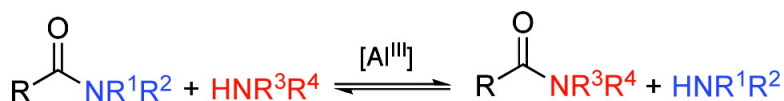


Discovery and Mechanistic Study of Al-Catalyzed Transamidation of Tertiary Amides

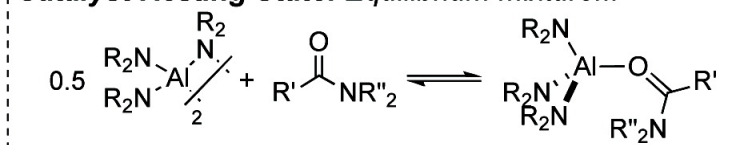
Justin M. Hoerter, Karin M. Otte, Samuel H. Gellman, Qiang Cui, and Shannon S. Stahl

J. Am. Chem. Soc., 2008, 130 (2), 647-654 • DOI: 10.1021/ja0762994

Downloaded from <http://pubs.acs.org> on February 8, 2009



Catalyst Resting State: Equilibrium mixture...



More About This Article

Additional resources and features associated with this article are available within the HTML version:

- Supporting Information
- Links to the 4 articles that cite this article, as of the time of this article download
- Access to high resolution figures
- Links to articles and content related to this article
- Copyright permission to reproduce figures and/or text from this article

[View the Full Text HTML](#)

Discovery and Mechanistic Study of Al^{III}-Catalyzed Transamidation of Tertiary Amides

Justin M. Hoerter, Karin M. Otte, Samuel H. Gellman,* Qiang Cui,* and Shannon S. Stahl*

Department of Chemistry, University of Wisconsin—Madison, 1101 University Avenue, Madison, Wisconsin 53706

Received August 24, 2007; E-mail: gellman@chem.wisc.edu; cui@chem.wisc.edu; stahl@chem.wisc.edu

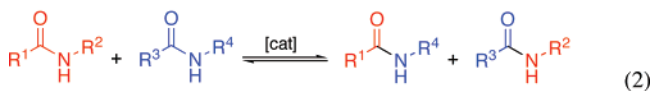
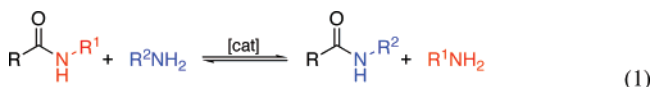
Abstract: Cleavage of the C–N bond of carboxamides generally requires harsh conditions. This study reveals that tris(amido)Al^{III} catalysts, such as Al₂(NMe₂)₆, promote facile equilibrium-controlled transamidation of tertiary carboxamides with secondary amines. The mechanism of these reactions was investigated by kinetic, spectroscopic, and density functional theory (DFT) computational methods. The catalyst resting state consists of an equilibrium mixture of a tris(amido)Al^{III} dimer and a monomeric tris(amido)Al^{III}–carboxamide adduct, and the turnover-limiting step involves intramolecular nucleophilic attack of an amido ligand on the coordinated carboxamide or subsequent rearrangement (intramolecular ligand substitution) of the tetrahedral intermediate. Fundamental mechanistic differences between these tertiary transamidation reactions and previously characterized transamidations involving secondary amides and primary amines suggest that tertiary amide/secondary amine systems are particularly promising for future development of metal-catalyzed amide metathesis reactions that proceed via transamidation.

Introduction

“Dynamic covalent chemistry” (DCC) has gained widespread attention as a means of preparing organic molecules and materials under thermodynamic, rather than kinetic, control.¹ Successful applications of DCC have been demonstrated with a variety of functional groups,² including esters, thioesters, imines, disulfides, and alkenes.³ The exchange reactions involving these functional groups are achieved through the use of an

appropriate catalyst that promotes facile formation and cleavage of the respective covalent bonds (Figure 1).

The diversity and significance of carboxamide-containing molecules in chemistry and biology suggest that amide-exchange reactions, including transamidation and amide metathesis (eqs 1 and 2), could have broad utility in DCC applications.



In contrast to the examples in Figure 1, however, methods for catalytic exchange of carboxamide C–N bonds suitable for DCC applications are not readily available.^{4–6} This deficiency underlies our recent efforts to develop catalysts that promote these reactions.⁷

We recently reported the first catalysts capable of promoting transamidation of secondary amides with primary amines under

- (1) Reviews of dynamic covalent chemistry: (a) Lehn, J.-M. *Chem. Eur. J.* **1999**, *5*, 2455–2463. (b) Rowan, S. J.; Cantrill, S. J.; Cousins, G. R. L.; Sanders, J. K. M.; Stoddart, J. F. *Angew. Chem., Int. Ed.* **2002**, *41*, 898–952. (c) Corbett, P. T.; Leclaire, J.; Vial, L.; West, K. R.; Wietor, J.-L.; Sanders, J. K. M.; Otto, S. *Chem. Rev.* **2006**, *106*, 3652–3711.
- (2) For selected recent applications of dynamic covalent chemistry, see: (a) Brady, P. A.; Bonar-Law, R. P.; Rowan, S. J.; Suckling, C. J.; Sanders, J. K. M. *Chem. Commun.* **1996**, 319–320. (b) Oh, K.; Jeong, K.-S.; Moore, J. S. *Nature* **2001**, *414*, 889–893. (c) Otto, S.; Furlan, R. L. E.; Sanders, J. K. M. *Science* **2002**, *297*, 590–593. (d) Kilbinger, A. F. M.; Cantrill, S. J.; Waltman, A. W.; Day, M. W.; Grubbs, R. H. *Angew. Chem., Int. Ed.* **2003**, *42*, 3281–3285; *Angew. Chem.* **2003**, *115*, 3403–3407. (e) Vignon, S. A.; Thibaut, J.; Iijima, T.; Tseng, H.-R.; Sanders, J. K. M.; Stoddart, J. F. *J. Am. Chem. Soc.* **2004**, *126*, 9884–9885. (f) Cantrill, S. J.; Grubbs, R. H.; Lanari, D.; Leung, K. C.-F.; Nelson, A.; Poulin-Kerstien, K. G.; Smidt, S. P.; Stoddart, J. F.; Tirrell, D. A. *Org. Lett.* **2005**, *7*, 4213–4216. (g) Cacciapaglia, R.; Di Stefano, S.; Mandolini, L. *J. Am. Chem. Soc.* **2005**, *127*, 13666–13671. (h) Shi, B.; Stevenson, R.; Campopiano, D. J.; Greaney, M. F. *J. Am. Chem. Soc.* **2006**, *128*, 8459–8467. (i) Vial, L.; Ludlow, R. F.; Leclaire, J.; Pérez-Fernández, R.; Otto, S. *J. Am. Chem. Soc.* **2006**, *128*, 10253–10257. (j) Dirksen, A.; Dirksen, S.; Hackeng, T. M.; Dawson, P. E. *J. Am. Chem. Soc.* **2006**, *128*, 15602–15603.
- (3) For representative fundamental studies of equilibrium-controlled exchange of covalent bonds, see ref 1 and the following: (a) Stanton, M. G.; Allen, C. B.; Kissling, R. M.; Lincoln, A. L.; Gagné, M. R. *J. Am. Chem. Soc.* **1998**, *120*, 5981–5989. (b) Nyce, G. W.; Lamboy, J. A.; Connor, E. F.; Waymouth, R. M.; Hedrick, J. L. *Org. Lett.* **2002**, *4*, 3587–3590. (c) Ong, T.-G.; Yap, G. P. A.; Richeson, D. S. *Chem. Commun.* **2003**, 2612–2613. (d) Singh, R.; Kissling, R. M.; Letellier, M.-A.; Nolan, S. P. *J. Org. Chem.* **2004**, *69*, 209–212. (e) Trnka, T. M.; Grubbs, R. H. *Acc. Chem. Res.* **2001**, *34*, 18–29. (f) Dirksen, A.; Hackeng, T. M.; Dawson, P. E. *Angew. Chem., Int. Ed.* **2006**, *45*, 7581–7584.

- (4) Transamidation at very high temperatures (>250 °C), typically with polyamides, has been reported: (a) Smith, M. E.; Adkins, H. *J. Am. Chem. Soc.* **1938**, *60*, 657–663. (b) Beste, L. F.; Houtz, R. C. *J. Polym. Sci.* **1952**, *8*, 395–407. (c) Ogata, N. *Makromol. Chem.* **1959**, *30*, 212–224. (d) Miller, I. K. *J. Polym. Sci., Part A: Polym. Chem.* **1976**, *14*, 1403–1417. (e) McKinney, R. J. U.S. Patent 5,302,756, 1994. (f) McKinney, R. J. U.S. Patent 5,395,974, 1995.
- (5) For enzymatic approaches to secondary amide exchange reactions, see: (a) Sergeeva, M. V.; Mozhaev, V. V.; Rich, J. O.; Khmelnskiy, Y. L. *Biotechnol. Lett.* **2000**, *22*, 1419–1422. (b) Swann, P. G.; Casanova, R. A.; Desai, A.; Frauenhoff, M. M.; Urbancic, M.; Slomczynska, U.; Hopfinger, A. J.; Le Breton, G. C.; Venton, D. L. *Biopolymers* **1996**, *40*, 617–625.

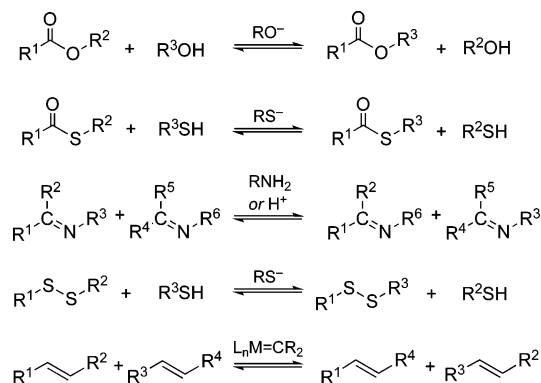
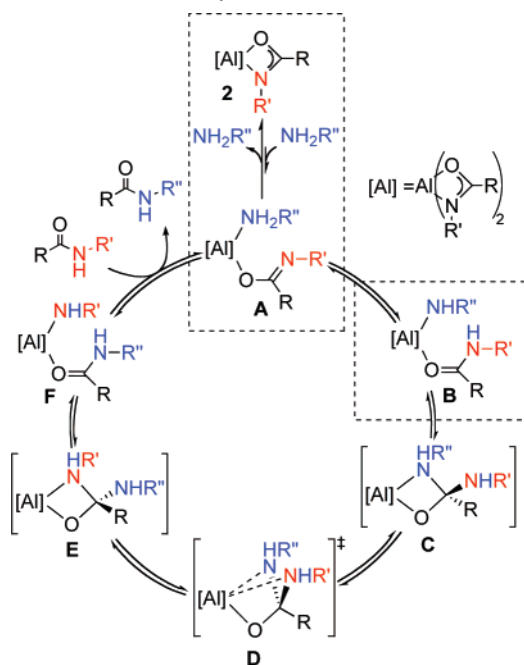


Figure 1. Self-exchange reactions that have been applied to dynamic covalent chemistry (DCC) applications.

Scheme 1. Proposed Mechanism for Al^{III}-Catalyzed Transamidation of Secondary Amides



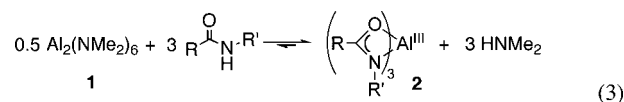
moderate conditions (eq 1).^{7a} One of the most effective catalysts for these reactions proved to be the homoleptic amidoaluminum complex $\text{Al}_2(\text{NMe}_2)_6$ (**1**). Subsequent mechanistic studies revealed that this dimeric Al complex is actually a “precatalyst”. Under the reaction conditions, it reacts rapidly with 3 equiv of

Table 1. Catalytic Transamidation of Tertiary Amides with Secondary Amides^a

Entry	R	NR ¹ R ²	NR ³ R ⁴	Amide Percent (I/II) ^b	
				Forward	Reverse
1	<i>n</i> -C ₆ H ₁₃			39/59	37/59
2	<i>n</i> -C ₆ H ₁₃			46/53	44/54
3	<i>n</i> -C ₆ H ₁₃			58/35	60/34
4				41/54	37/58
5				39/68	37/61
6				56/40	55/41

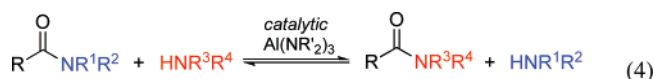
^a Reaction conditions: $[\text{Al}_2(\text{NMe}_2)_6] = 4.3 \text{ mM}$, $[\text{carboxamide}] = 0.17 \text{ M}$, $[\text{amine}] = 0.17 \text{ M}$, 2 mL of toluene, 90 °C, 16 h. ^b Determined by GC (internal standard = triphenylmethane); data represent the average of two reactions. Formation of N,N-dimethylcarboxamide product was observed in ~5% yield; the remaining amide products were I and II in each case.

secondary carboxamide to form a tris(amide)Al^{III} species (**2**) (eq 3).⁸



Kinetic and NMR-spectroscopic studies revealed that complexes of this type represent the resting state of Al^{III} during catalytic turnover and that the tris(κ^2 -amide)Al^{III} complexes enter the catalytic cycle via a bimolecular reaction with a primary amine substrate (**2** + RNH₂ → **A**, Scheme 1).

The insights from this mechanistic study suggested that more efficient catalysis could be achieved by destabilizing the tris(κ^2 -amide)Al^{III} species, thereby making it more reactive, or by circumventing this species altogether. Tertiary carboxamides lack an acidic N–H group and cannot form the amide–aluminum species. Therefore, tertiary amides could react directly with tris(amido)Al^{III} complexes to form a species analogous to intermediate **B** in Scheme 1 and undergo efficient transamidation (eq 4).



Here, we validate this hypothesis by demonstrating the first examples of tertiary amide transamidation catalysis. The mech-

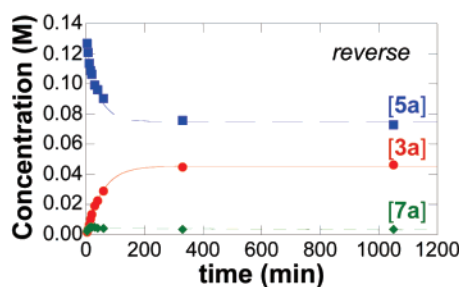
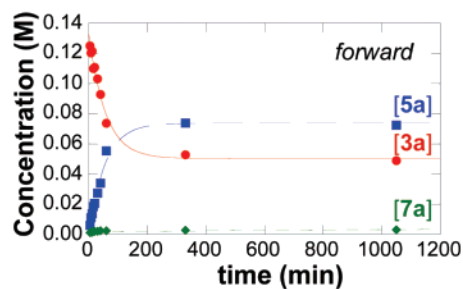
(6) Precedents for transamidation under synthetically practical conditions are typically limited to intramolecular reactions or require a stoichiometric reagent: (a) Galat, A.; Elion, G. *J. Am. Chem. Soc.* **1943**, *65*, 1566–1567. (b) Martin, R. B.; Parcell, A.; Hedrick, R. I. *J. Am. Chem. Soc.* **1964**, *86*, 2406–2413. (c) Crombie, L.; Jones, R. C. F.; Haigh, D. *Tetrahedron Lett.* **1986**, *27*, 5151–5154. (d) Zaragoza-Dörwald, F.; von Kiedrowski, G. *Synthesis* **1988**, *11*, 917–918. (e) Gotor, V.; Brieva, R.; González, C.; Rebollo, F. *Tetrahedron* **1991**, *47*, 9207–9214. (f) Bon, E.; Bigg, D. C. H.; Bertrand, G. *J. Org. Chem.* **1994**, *59*, 4035–4036. (g) Suggs, J. W.; Pires, R. M. *Tetrahedron Lett.* **1997**, *38*, 2227–2230. (h) Langlois, N. *Tetrahedron Lett.* **2002**, *43*, 9531–9533. (i) Lasri, J.; González-Rosende, M. E.; Sepúlveda-Arques, J. *Org. Lett.* **2003**, *5*, 3851–3853. (j) Klapars, A.; Parris, S.; Anderson, K. W.; Buchwald, S. L. *J. Am. Chem. Soc.* **2004**, *126*, 3529–3533. (k) Alajarín, M.; Vidal, A.; Tovar, F. *Tetrahedron* **2005**, *61*, 1531–1537. (l) Çalimsiz, S.; Lipton, M. A. *J. Org. Chem.* **2005**, *70*, 6218–6221. (m) Dineen, T. A.; Zajac, M. A.; Myers, A. G. *J. Am. Chem. Soc.* **2006**, *128*, 16406–16409.

(7) (a) Eldred, S. E.; Stone, D. A.; Gellman, S. H.; Stahl, S. S. *J. Am. Chem. Soc.* **2003**, *125*, 3422–3423. (b) Bell, C. M.; Kissounko, D. A.; Gellman, S. H.; Stahl, S. S. *Angew. Chem., Int. Ed.* **2007**, *46*, 761–763. See also: (c) Shi, M.; Cui, S.-C. *Synth. Commun.* **2005**, *35*, 2847–2858.

(8) Hoerter, J. M.; Otte, K. M.; Gellman, S. H.; Stahl, S. S. *J. Am. Chem. Soc.* **2006**, *128*, 5177–5183.

(9) The stoichiometric formylation of amines with *N,N*-dimethylformamide has been reported: (a) Pettit, G. R.; Thomas, E. G. *J. Org. Chem.* **1959**, *24*, 895–896. (b) Pettit, G. R.; Kalnins, M. V.; Liu, T. M. H.; Thomas, E. G.; Parent, K. J. *J. Org. Chem.* **1961**, *26*, 2563–2566. (c) Kraus, M. A. *Synthesis* **1973**, 361–362.

A. Heptanamide Transamidation



B. Toluamide Transamidation

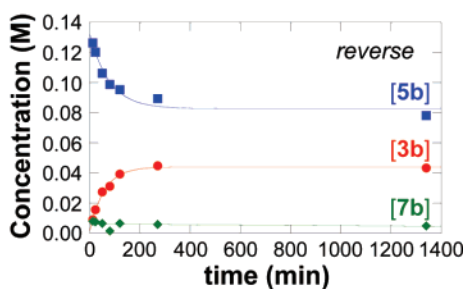
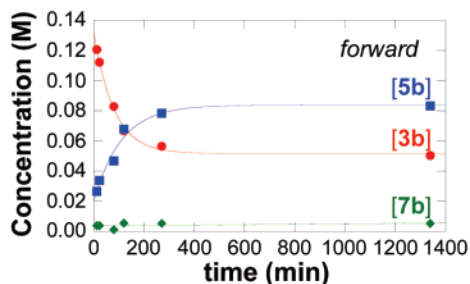


Figure 2. Representative time-courses for Al₂(NMe₂)₆-catalyzed transamidation between **3a** and **4** (A) and **3b** and **4** (B) in both the forward and reverse directions. Conditions: [Al₂(NMe₂)₆] = 4.3 mM, [carboxamide] = 0.17 M, [amine] = 0.17 M, 5 mL of toluene, 90 °C.

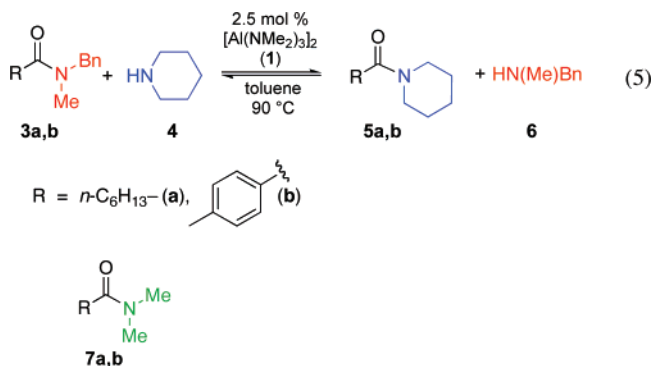
anism of these reactions is investigated by experimental and computational methods. The results highlight similarities and differences between Al^{III}-catalyzed transamidation of secondary and tertiary carboxamides and suggest opportunities for the development of improved catalysts.

Results and Discussion

Al^{III}-Catalyzed Tertiary Amide Transamidation. This study was initiated by evaluating whether the amidoaluminum complex Al₂(NMe₂)₆ (**1**) could catalyze the transamidation of tertiary amides. We selected tertiary amide/secondary amine pairs that should be approximately thermoneutral (Table 1). Conditions analogous to those used in the transamidation of secondary amides were employed: 5 mol % [Al] (2.5 mol % [**1**]) in toluene as the solvent at 90 °C. The reactions were performed in both forward and reverse directions, as shown in Table 1, and achievement of equilibrium was demonstrated when an identical product ratio was obtained for the forward and reverse reactions. The data in Table 1 indicate that equilibrium was attained for each of the six substrate pairs examined. Small amounts of the *N,N*-dimethylcarboxamide (~5%) were observed in each reaction mixture, resulting from incorporation of the dimethylamino fragment of **1** into the amide products. To our knowledge, these results represent the first examples of catalytic equilibration of tertiary amide-secondary amine mixtures.⁹ Following these initial demonstrations of catalytic reactivity, we undertook mechanistic studies to probe the similarities and differences between Al^{III}-catalyzed transamidation of secondary versus tertiary amides.

Kinetic Studies of Al^{III}-Catalyzed Transamidation of Tertiary Toluamides. Mechanistic studies of Al^{III}-catalyzed transamidation between secondary amines and tertiary carboxamides were initiated by identifying substrates that could be monitored readily by NMR spectroscopy and/or gas chromatography. The substrate pairs *N*-benzyl-*N*-methylheptanamide

(**3a**)/piperidine (**4**) and *N*-benzyl-*N*-methyl-*p*-toluamide (**3b**)/piperidine (**4**) proved suitable for this purpose (eq 5).



In the presence of 2.5 mol % Al₂(NMe₂)₆ (**1**) in toluene at 90 °C, these substrate pairs react to produce an equilibrium mixture of carboxamides **3** and **5** and amines **4** and **6** (Figure 2). Identical product ratios were obtained when the reactions were performed in the forward or reverse directions, which establishes that the reactions reached equilibrium. A small amount of *N,N*-dimethylcarboxamide product (**7**) was detected in each of the reaction mixtures.

Initial-rate kinetic methods were used to examine the dependence of the reaction rate on each of the components, Al₂(NMe₂)₆, amine, and carboxamide. The reaction rate was obtained by monitoring the carboxamide concentrations by gas chromatography during the first 5% conversion of the starting materials. The initial-rate dependence on [Al₂(NMe₂)₆] was monitored over a range of 1–10 mol % of **1** (2–20 mol % monomeric Al^{III}), and the rates were measured at different concentrations of the substrates, carboxamide **3a** and amine **4** (Figure 3). A saturation dependence of the rate on [**1**] and [**3a**] was observed, but the rate was unaffected by changes in the

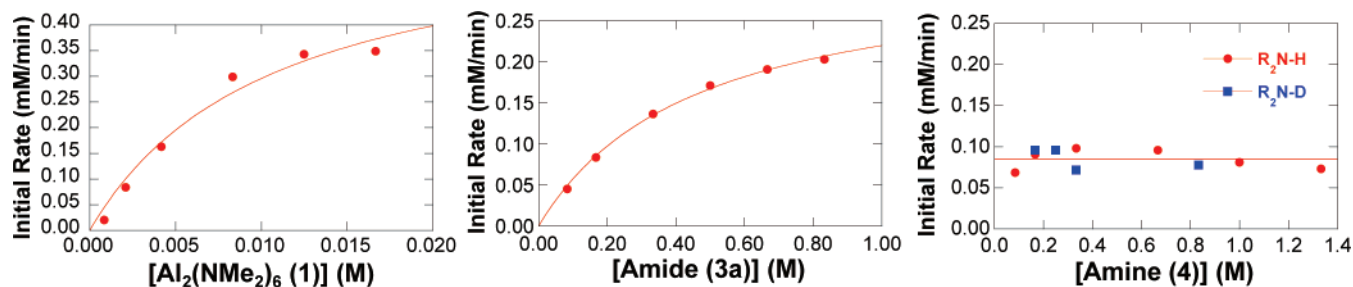


Figure 3. Kinetic data for $\text{Al}_2(\text{NMe}_2)_6$ -catalyzed transamidation of heptanamide **3a** with piperidine **4**. The [Al]- and [amide]-dependence data were fit to a generic hyperbolic function (i.e., saturation dependence), and the line in the [amine]-dependence plot reflects a zero-order fit. Standard reaction conditions: $[\mathbf{1}] = 2.1 \text{ mM}$; $[\mathbf{3a}] = [\mathbf{4}] = 0.17 \text{ M}$, 5 mL of toluene, 90 °C.

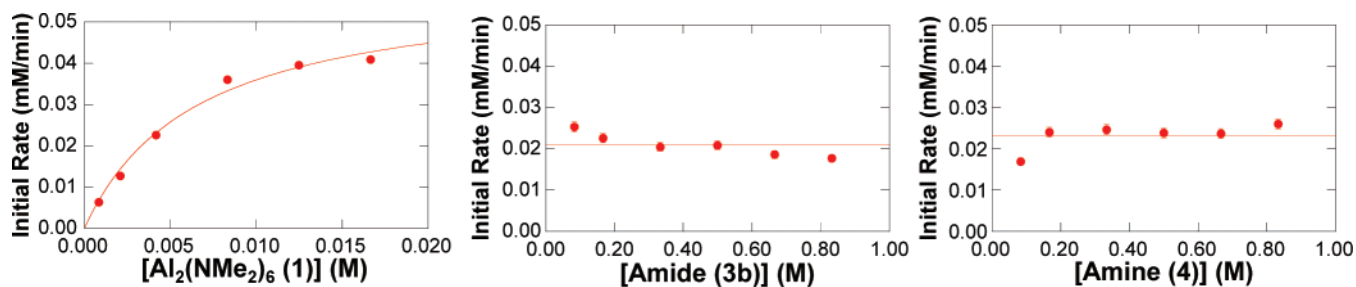


Figure 4. Kinetic data for $\text{Al}_2(\text{NMe}_2)_6$ -catalyzed transamidation of toluamide **3b** with piperidine **4**. The Al-dependence data was fit to a generic hyperbolic function (i.e., saturation dependence), and the lines in the amide- and amine-dependence plots reflect a zero-order fit. Standard reaction conditions: $[\mathbf{1}] = 4.3 \text{ mM}$; $[\mathbf{3b}] = [\mathbf{4}] = 0.17 \text{ M}$, 5 mL of toluene, 90 °C.

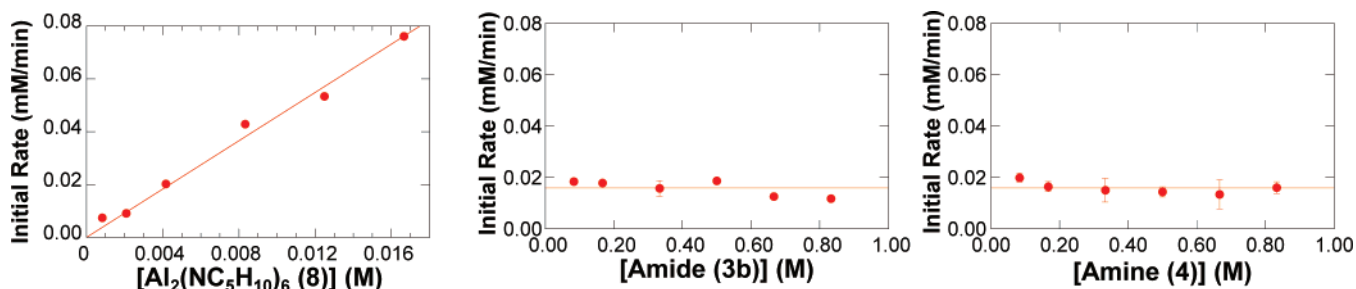
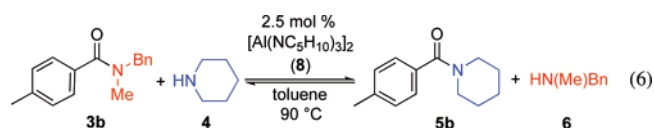


Figure 5. Kinetic data for $\text{Al}_2(\text{NMe}_2)_6$ -catalyzed transamidation of toluamide **3b** with piperidine **4**. (The quantity of piperidine (**4**) used in each reaction was adjusted to account for the aluminum-bound piperidido groups in order to maintain a 1:1 ratio of amino groups derived from piperidine and benzylmethylamine. For example, with a 2.5 mol % loading of $\text{Al}_2(\text{NC}_5\text{H}_{10})_6$, the quantity of piperidine was reduced by 15% relative to **3**.) The curve-fit of the Al-dependence data reflects a linear least-squares fit of the data, and the lines in the amide- and amine-dependence plots reflect a zero-order fit. Standard reaction conditions: $[\mathbf{8}] = 4.3 \text{ mM}$; $[\mathbf{3b}] = [\mathbf{4}] = 0.17 \text{ M}$; 5 mL of toluene, 90 °C.

amine concentration. No deuterium kinetic isotope effect was observed when the *N*-deuterated amine was used as the substrate.

Kinetic studies of transamidation of the toluamide substrate **3b** (Figure 4) revealed some differences relative to those with heptanamide substrate **3a**. The overall rates of toluamide transamidation were 5–10-fold slower than those with **3a**, depending on the reaction conditions. The kinetic data revealed a saturation dependence on the catalyst concentration, **[1]**, but changes to the amide and amine concentrations had no effect on the rate.

In order to avoid the formation of **7**, we prepared the tris(piperidido)–Al^{III} complex $\text{Al}_2(\text{NC}_5\text{H}_{10})_6$ (**8**)¹⁰ and investigated its use as a catalyst for transamidation between **3b** and **4** (eq 6). Kinetic studies of this reaction revealed that the



(10) Passarelli, V.; Carta, G.; Rossetto, G.; Zanella, P. *Dalton Trans.* **2003**, 1284–1291.

transamidation rate exhibits a linear, first-order dependence on **[8]** (Figure 5). No rate dependence on [amine] or [carboxamide] was observed (Figure 5).

Spectroscopic Studies of Al^{III}-Catalyzed Transamidation.

¹H NMR spectroscopy was employed to probe the degenerate transamidation (self-exchange) of *N,N*-dimethyltoluamide (**7b**) with dimethylamine under typical catalytic conditions (toluene-*d*₈, 90 °C).¹¹ Spectra of the individual reaction components, $\text{Al}_2(\text{NMe}_2)_6$ (**1**), **7b**, and Me_2NH , are shown in Figure 6A–C. The catalyst, **1**, exists as a dimer at 90 °C, as revealed by the separate resonances for the bridging and terminal dimethylamido ligands (2.39 and 2.67 ppm, respectively; Figure 6A). Addition of 5 equiv of Me_2NH to a solution of **1** results in broadening of the resonances associated with both species. The resonances for the terminal and bridging dimethylamido ligands of **1** remain separate (Figure 6D). In contrast, addition of carboxamide **7b** to **1** results in coalescence of the resonances for terminal and bridging dimethylamido ligands (Figure 6E); the chemical shift

(11) ¹H NMR spectra of cross-exchange reaction solutions, such as that initially containing **3b** and **4**, proved to be too complex to identify all of the various species present.

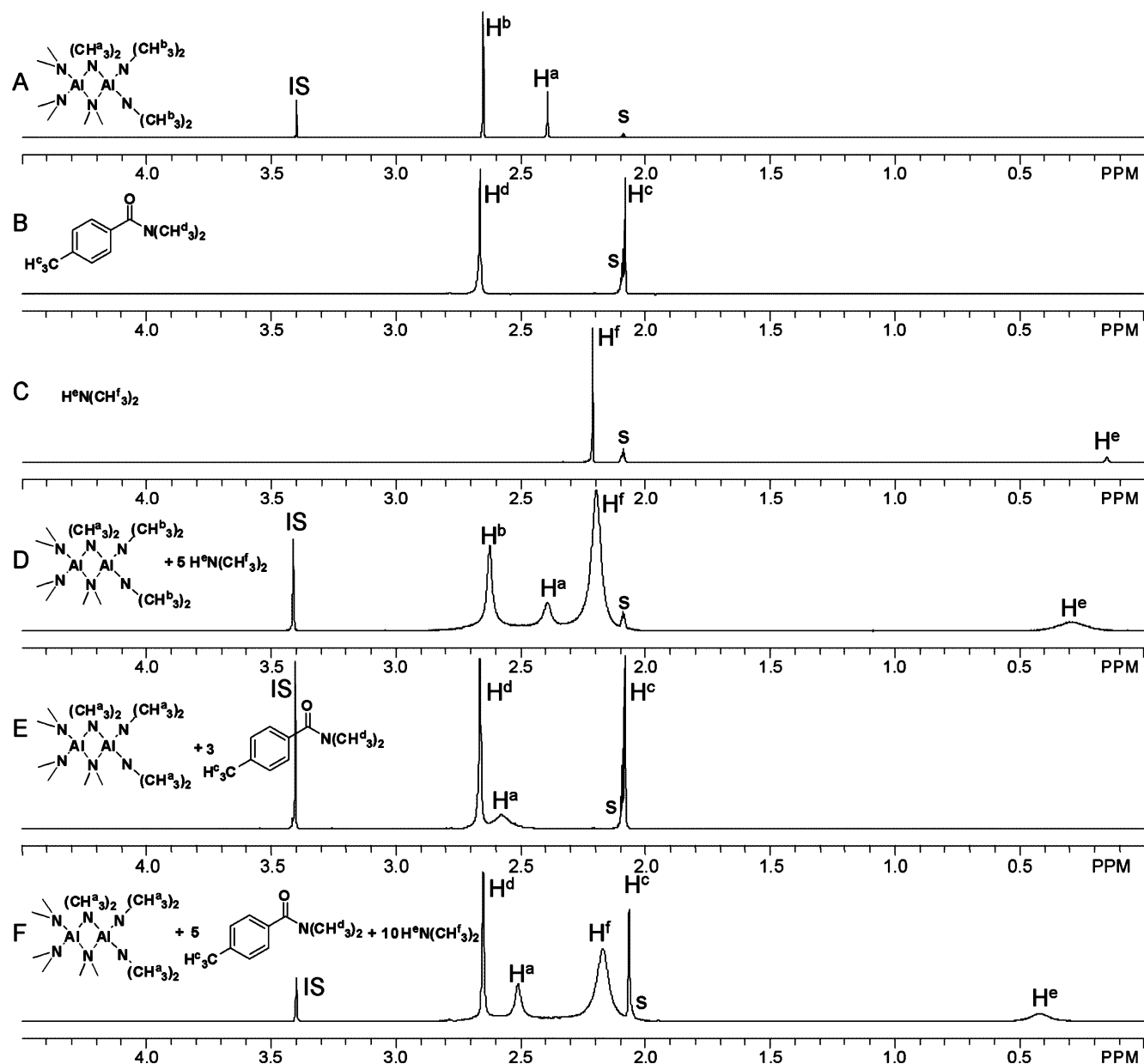
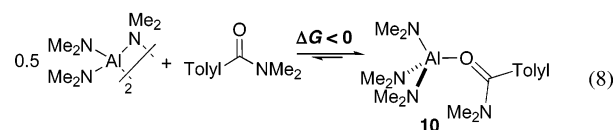


Figure 6. NMR spectra relevant to Al^{III}-catalyzed transamidation of tertiary amides. All spectra were acquired at 90 °C in toluene-*d*₈. (IS = internal standard = trimethoxybenzene; S = solvent = toluene-*d*₈.)

of the broad dimethylamido resonance at 2.57 ppm corresponds to the weighted average of the chemical shifts for the terminal and bridging amido ligands. This result implies that the dimethylamido ligands of **1** undergo facile exchange between terminal and bridging coordination sites in the presence of **7b**. The peaks associated with the methyl groups of **7b**, (CH₃)₂N– and Ar–CH₃ (2.67 and 2.08 ppm, respectively), remain sharp, and their chemical shifts are essentially unchanged. When all three reaction components (**1**, **7b**, and Me₂NH) are present in solution the CH₃– resonances of dimethylamine are broad, but the chemical shift is unchanged relative to the two-component mixture (**1** + Me₂NH; Figure 6D). Sharp peaks are observed for **7b** (as in the mixture of **1** and **7b**; Figure 6E), but the single broad peak associated with dimethylamido ligands coordinated to Al is shifted upfield (2.51 ppm) relative to the peak observed in the two-component mixture of **1** and **7b** (2.57 ppm).

These spectroscopic data suggest that the amine and carboxamide substrates are capable of reversible coordination to

the Al centers of **1** (eqs 7 and 8). Broadening of the resonances



of **1** and dimethylamine in Figure 6D can arise from coordination of Me₂NH to the Al centers to form the monomeric (Me₂N)₃Al–NHMe₂ species (**9**) (eq 7), a process that will promote exchange between the terminal and bridging dimethylamido ligands in **1**. The observation of separate resonances for the terminal and bridging dimethylamido ligands in this spectrum suggests that equilibrium coordination of Me₂NH to **1**

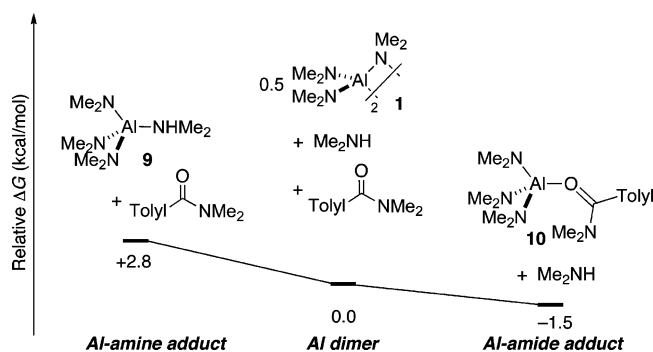


Figure 7. Relative free energies (kcal/mol) of $\text{Al}_2(\text{NMe}_2)_6$ (**1**) and the corresponding Al-amine and Al-amide adducts (**9** and **10**, respectively) derived from DFT calculations.

favors the separated reagents (**1** + Me_2NH , eq 7) and is relatively slow on the NMR time scale. In the mixture of carboxamide **7b** and **1**, coalescence of the resonances for terminal and bridging amido ligands of **1** suggests that coordination of **7b** to **1** is rapid on the NMR time scale (eq 8). Moreover, in the three-component mixture (**1** + **7b** + Me_2NH ; Figure 6F), the upfield chemical shift of the Al-bound dimethylamido ligands relative to the weighted average of the chemical shifts for the terminal and bridging dimethylamido ligands is consistent with population of a new Al species, presumably the Al-carboxamide adduct $(\text{Me}_2\text{N})_3\text{Al}-\text{O}=\text{C}(\text{tolyl})(\text{NMe}_2)$ (**10**) (eq 8). The latter assignment remains tentative because no changes are evident to the $\text{N}-\text{CH}_3$ resonances of the carboxamide, and it is not obvious how the presence of amine shifts the position of the equilibrium involving coordination of the carboxamide to **1**.¹² The experimental assignment is supported, however, by the computational studies described below.

Computational Studies of Al^{III}-Catalyzed Transamidation.

Density functional theory (DFT) calculations were used to evaluate the energies of proposed intermediates as well as the reaction coordinate for Al-catalyzed transamidation of tertiary amides. The free energies of dimeric Al complex **1** and the monomeric substrate adducts **9** and **10** were calculated to probe the origin of the NMR spectroscopic data described above (Figure 7). The results indicate that coordination of Me_2NH to the Al center is slightly disfavored energetically, $\Delta G = +2.8$ kcal/mol, relative to **1** and free amine, whereas coordination of carboxamide **7b** to Al is slightly favored, $\Delta G = -1.5$ kcal/mol. These results support the conclusions derived from the spectroscopic data described above.

The identity of the carboxamide influences the stability of the Al-coordinated adduct. Coordination of *N*-piperidinyltoluamide to $\text{Al}(\text{NMe}_2)_3$ is calculated to be slightly favored thermodynamically with respect to the dimeric Al complex **1** ($\Delta G = -1.3$ kcal, Figure 8). In contrast, coordination of *N*-piperidinylheptanamide to Al is slightly disfavored ($\Delta G = +0.3$ kcal/mol). The relative stability of these two carboxamide adducts probably accounts for the kinetic results in Figures 3 and 4, which indicate that the rate of transamidation exhibits a saturation dependence on the heptanamide **3a** but a zero-order dependence on the toluamide **3b** (see further discussion below).

A simplified transamidation model system, consisting of *N,N*-dimethylacetamide and dimethylamine as the substrates, was

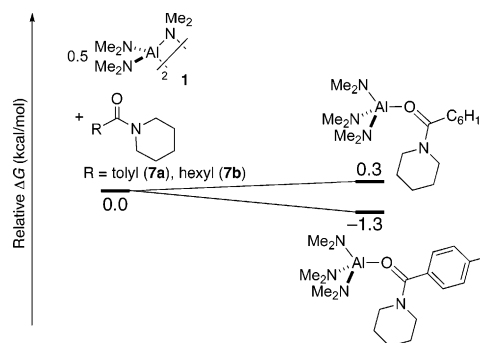


Figure 8. Relative free energies (kcal/mol) of $\text{Al}_2(\text{NMe}_2)_6$ (**1**) and the adducts arising from coordination of carboxamides **7a** and **7b** to $\text{Al}(\text{NMe}_2)_3$ derived from DFT calculations. See the Experimental Section for computational details.

used to probe the reaction profile for Al-catalyzed transamidation of tertiary amides. Coordination of *N,N*-dimethylacetamide to Al provides a means of activating the carboxamide substrate, and the acetamide adduct $(\text{Me}_2\text{N})_3\text{Al}-\text{O}=\text{C}(\text{NMe}_2)\text{Me}$ (**A**) is calculated to have a free energy 2.7 kcal/mol higher than the dimeric Al complex **1**.¹³ Nucleophilic attack of a coordinated dimethylamido ligand on the bound acetamide yields metallacyclic intermediate **12** via transition state **TS1**. Transamidation occurs by interchange of the $\text{Me}_2\text{N}-$ fragments in **12** via transition state **TS2**, which is the highest-energy species on the reaction coordinate. No interaction is detected between the Al center, and the two N atoms in **TS2**; the Al...N bond distances in this structure are 3.05 Å.

The 28.4 kcal/mol calculated activation barrier for Al-catalyzed transamidation (Figure 9) compares favorably with activation barriers determined experimentally. For example, $\text{Al}_2(\text{NMe}_2)_6$ -catalyzed transamidation of **3a** and **4** exhibits a free energy of activation (ΔG^\ddagger) of 31.0 kcal/mol ($[\mathbf{1}] = 4.3$ mM, Figure 3). The 2.6 kcal/mol difference between the calculated and experimental activation energies is quite reasonable in light of our observation that substrate structure can have a significant influence on the rate of transamidation (e.g., compare data in Figures 3 and 4).

Proposed Catalytic Mechanism and Analysis of Mechanistic Data. A catalytic cycle consistent with the data presented above is shown in Scheme 2. Coordination of the carboxamide substrate to Al results in cleavage of dimer **A** and formation of the monomeric Al-carboxamide adduct **B**. Nucleophilic attack of an amido ligand on the coordinated carboxamide in **B** yields the Al-stabilized tetrahedral intermediate **C**, and transamidation occurs by interchange of the two dialkylamino fragments (**C** → **C'**) via transition state **D**. Subsequent formation of the alternate carboxamide adduct **B'**, followed by substitution of the coordinated carboxamide and exchange of amido ligands, completes the catalytic cycle.

The catalyst resting state is species **A**, **B**, or a mixture of the two. These complexes appear to be nearly isoenergetic, with their relative stability depending upon the identity of the carboxamide, the amido ligands coordinated to Al, and the reaction conditions (e.g., the Al concentration). The equilibrium between **A** and **B**, as well as the ligand substitution steps

(13) Dissociation of **1** into monomeric $\text{Al}(\text{NMe}_2)_3$ is calculated to be uphill by only 5.2 kcal/mol. Therefore, formation of the Al-carboxamide adduct **11** probably occurs by a dissociation of **1** into 2 equiv of $\text{Al}(\text{NMe}_2)_3$ followed by coordination of the carboxamide to the three-coordinate Al center.

(12) Additional spectroscopic data is provided in the Supporting Information.

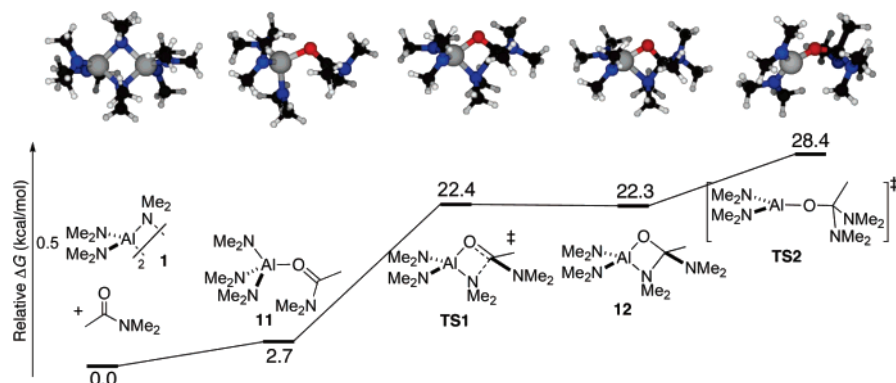
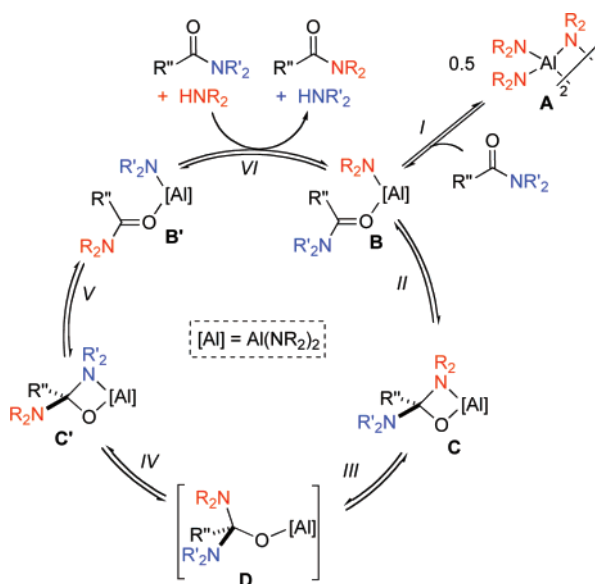


Figure 9. Calculated free energy profile (kcal/mol) for degenerate transamidation of *N,N*-dimethylacetamide mediated by $\text{Al}(\text{NMe}_2)_3$ derived from DFT calculations.

Scheme 2. Proposed Mechanism for Al^{III} -Catalyzed Transamidation



involved in the interconversion between **B'** and **B**, proceed rapidly relative to formation of the tetrahedral intermediate, **B** \rightarrow **C**, and interchange of the dialkylamino fragments of tetrahedral intermediate, **C** \rightarrow **C'**.

The proposed mechanism accounts for the different kinetic dependence on $[\text{Al}]$ in different transamidation reactions (Figures 3–5). The rate should exhibit a first-order dependence on $[\text{Al}]$ if monomeric species **B** is the catalyst resting state but a half-order dependence if **A** is the resting state. If the resting state consists of a mixture of monomeric and dimeric Al species, an intermediate dependence on $[\text{Al}]$ is expected. The nonlinear rate dependence on $[\text{Al}]$ in the transamidation reactions with $\text{Al}_2(\text{NMe}_2)_3$ as the catalyst (Figures 3 and 4) is intermediate between first- and half-order in $[\text{Al}]$, implying that a mixture of monomeric and dimeric Al species is present.¹⁴ In contrast, the transamidation reaction with piperidido–Al complex **8** as the catalyst (Figure 5) exhibits a first-order dependence on $[\text{Al}]$, consistent with a monomeric catalyst resting state. These differences in the nature of the catalyst resting state for different reactions presumably reflect the different ligands coordinated to Al. For example, the sterically more-demanding piperidido

ligands (relative to dimethylamido) could favor formation of a monomeric Al complex.

The [carboxamide]-dependence data can be analyzed similarly. The rate should exhibit a first-order dependence on [carboxamide] if the catalyst resting state is the Al dimer and a zero-order dependence if the resting state is the Al–carboxamide adduct. In one of the three reactions studied (Figure 3), the transamidation rate exhibits a saturation dependence on [carboxamide], and in the other two reactions, a zero-order dependence is observed (Figures 4 and 5). The saturation dependence reflects pre-equilibrium formation Al–carboxamide adduct, which favors of the carboxamide adduct at high [carboxamide].

The zero-order dependence of the transamidation rates on [amine] (Figures 3–5) reflects the fact that free amine does not participate in the turnover-limiting steps (**B** \rightarrow **C** \rightarrow **D**) of the catalytic reaction. An amido ligand coordinated to Al serves as the reactive nucleophile in the transamidation reaction, and amido ligand exchange with free amine is fast relative to the turnover rate.

Conclusion and Consideration of Broader Implications.

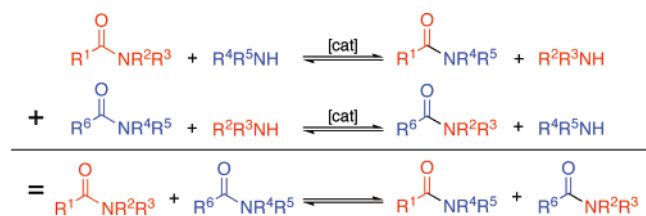
Analysis of the mechanism of Al-catalyzed transamidation of secondary amides⁸ suggested that tertiary amides would be effective transamidation substrates because they would prevent formation of stable amidate complexes with Al^{III} . In addition to validating this initial hypothesis by demonstrating the first examples of transamidation of tertiary amides, we have performed kinetic, spectroscopic, and computational studies to elucidate the mechanism of Al-catalyzed transamidation of tertiary amides. The results reveal both similarities and differences between secondary and tertiary carboxamides in catalytic transamidation reactions. The similarities are evident in the catalytic mechanisms (Schemes 1 and 2), which feature closely related fundamental steps and intermediates. For example, one of the key steps in both transformations is nucleophilic attack of an amido ligand on an Al-coordinated carboxamide. Perhaps the most important difference is the identity of the catalyst resting state, which leads to significant differences in the kinetic properties of the two reactions (Table 2).

The differences between secondary and tertiary transamidation reactions have important implications for the development of amide metathesis methods. Amide metathesis can potentially be achieved via successive transamidation reactions (Scheme 3). Efforts to promote secondary amide metathesis with Al

(14) A log–log plot of the $[\text{Al}]$ concentration data for these reactions exhibits a slope of ~ 0.6 , which reflects the approximate kinetic order in $[\text{Al}]$.

Table 2. Comparison of Secondary and Tertiary Transamidation Reactions

property	secondary amide transamidation	tertiary amide transamidation
catalyst resting state:		
kinetic order of catalytic rate law:		
[Al]	first-order	half-to-first-order
[carboxamide]	zero-order	zero-order or saturation
[amine]	first-order	zero-order

Scheme 3. Transamidation-Based Strategy to Achieve the Metathesis of 2° and 3° Carboxamides

transamidation catalysts were unsuccessful, however.^{15,16} Mechanistic studies later revealed the probable origin of this failure: the rate law for transamidation of 2° amides is first-order in [Al] and [amine], both of which will be low (or negligible, in the case of [amine]) in amide metathesis reactions. Furthermore, the only amide metathesis reagent present in high concentration is the carboxamide, but the rate law for secondary transamidations is zero-order in [carboxamide].

The kinetic properties of Al-catalyzed tertiary transamidation (Table 2) are quite distinct from those for secondary transamidation, and they appear compatible with a transamidation-based strategy for tertiary amide metathesis. Most importantly, the rate law for tertiary transamidation is zero-order in [amine]. The dependence of the rate on [Al] ranges from half- to first-order, and the dependence on [carboxamide] varies from zero-order to saturation behavior. On the basis of these observations, we are currently pursuing the development of tertiary amide metathesis reactions. An important goal of this ongoing work is the identification of improved transamidation catalysts. Most DCC applications utilize noncovalent interactions to bias the thermodynamic preference for a particular product among an equilibrium mixture, and optimal implementation of amide-exchange catalysis in DCC applications will require the identification of catalysts that operate at lower temperatures.

Experimental Section

General. All syntheses and sample preparations were performed using Schlenk techniques or in a nitrogen atmosphere glovebox. Toluene-*d*₈ was dried over sodium and benzophenone and distilled prior to use. Other solvents were dried with activated alumina purification columns. NMR spectral data were obtained using a Varian Unity 500

- (15) Lee, S. E.; Gellman, S. H.; Stahl, S. S. Unpublished results.
 (16) Successful development of secondary amide metathesis was achieved by employing an alternative, transacylation-based mechanism. See ref 7b.

MHz spectrometer. ¹H NMR spectra were referenced to residual C₆D₅-CD₂H (2.09 ppm). Gas chromatography was performed with a Shimadzu GC-17A gas chromatograph equipped with a 15 m RTX-5 capillary column (Restek). Al₂(NMe₂)₆ was purchased from Strem and used as received, and Al₂(NC₅H₆)₆ was prepared by using the literature procedure for the Al-pyrrolidine complex;¹⁰ characterization data matched the known compound.¹⁷

General Procedure for Kinetics Studies. The following representative procedure was used to obtain initial-rate data that are contained in Figures 3–5. Toluene stock solutions of aluminum catalyst **1** (41 mM, 0.66 g in 5.0 mL of toluene), amide **3b** (0.83 M, 1.99 g in 10.0 mL of toluene), amine **4** (0.83 M, 0.71 g in 10.0 mL of toluene), and internal standard triphenylmethane (0.42 M, 1.02 g in 10.0 mL of toluene) were prepared in the glovebox. In a 12-well temperature-controlled reactor (IKA RCT fitted with an IKA ETS-04 controller), 1.0 mL of each of the stock solutions for **3b**, **4**, and internal standard was premixed with 1.5 mL of toluene. The reaction was initiated by addition of 0.5 mL of the catalyst stock solution (5 mol % catalyst). The first 100 μL aliquot of the reaction mixture was withdrawn immediately upon mixing. Samples were collected every 2 min for initial-rate studies, and the reaction in each 100 μL aliquot was quenched by dilution of the aliquot in 2 mL of toluene at room temperature. The samples were analyzed by gas chromatography, and concentrations were determined by integration relative to the internal standard, triphenylmethane.

Representative NMR Spectroscopic Study. Stock solutions of **7b** (167 mM, 0.136 g in 2.0 mL of toluene-*d*₈), **1** (33 mM, 0.026 g in 2.0 mL of toluene-*d*₈), and internal standard 1,3,5-trimethoxybenzene (42 mM, 0.046 g in 2.0 mL of toluene-*d*₈) were prepared in a glovebox. Three NMR tubes were prepared with 40, 120, or 200 μL of **7b** (2, 6, and 10 equiv relative to **1**) and 200 μL each of solutions of **1** and internal standard. The solvent volume of each NMR tube was brought up to 0.5 mL with toluene-*d*₈ (360, 180, and 100 μL, respectively), and NMR spectra were acquired at 28 and 90 °C on a 500 MHz spectrometer.

DFT Calculations. Calculations were performed with the Gaussian 03 program¹⁸ and the Becke3LYP functional.¹⁹ Initial geometries were obtained using the lan12dz basis set followed by optimization and frequency analysis using the 6-31G(d,p) basis set for all atoms except Al, for which the lan12dz basis set with an additional a polarization function (ζ = 0.325) was used. Final total energies were obtained with the 6-311+G(d,p) on all atoms. The nature of all stationary points was confirmed by performing frequency analyses. For transition states, subsequent intrinsic reaction coordinate (IRC) calculations were performed to demonstrate their connection to the adjacent ground states. All quoted free energies include a correction for zero-point energies, and thermal contributions (within the rigid-rotor-harmonic-oscillator approximation) are adjusted to 363.15 K (90 °C).

Acknowledgment. We are grateful to the NSF Collaborative Research in Chemistry program (CHE-0404704) for financial support of this work.

Supporting Information Available: Complete ref 16, additional ¹H NMR spectroscopic data for mixtures of Al₂(NMe₂)₆, carboxamide, and amine, and Cartesian coordinates and energies for computed structures. This material is available free of charge via the Internet at <http://pubs.acs.org>.

JA0762994

- (17) Andrianarison, M. M.; Ellerby, M. C.; Gorrel, I. B.; Hitchcock, P. B.; Smith, J. D.; Stanley, D. R. *J. Chem. Soc., Dalton Trans.* **1996**, 211–217.
 (18) Frisch, M. J.; et al. *Gaussian 03*, revision B.04; Gaussian, Inc.: Pittsburgh, PA, 2004.
 (19) (a) Becke, A. D. *J. Chem. Phys.* **1993**, *98*, 1372–1377. (b) Lee, C. T.; Yang, W. T.; Parr, R. G. *Phys. Rev. B* **1988**, *37*, 785–789.